J Mol Model (2012) 18:4291–4298
DOI 10.1007/s00894-012-1438-8

ORIGINAL PAPER

Substituent effects on the properties of fluorene-thieno[3,4-b] pyrazine derivatives for light-emitting applications

Yanling Wang · Qiang Peng · Zaifang Li · Ping He · Benlin Li

Received: 23 December 2011 / Accepted: 17 April 2012 / Published online: 8 May 2012

Abstract Five thieno[3,4-b]pyrazine-based model compounds were studied to explore the effects of the substituent groups (alkyl or aryl) on the structure, atomic charge, optical properties, ionization potential (IP), electron affinity (EA), and reorganization energy. Theoretical calculations were carried out by density functional theory (DFT) using the B3LYP hybrid function combined and CAM-B3LYP with the 6-31G(d) basis set. The lowest-lying absorption and emission spectra of 9,9′-diethylhexylfluorene-alt-5,7-dithien-2-yl-thieno[3,4-b] pyrazine (FDDTTP) with alkyl groups showed a blue-shift, while those of FDDTTP with aryl groups exhibited a red-shift. The results agree well with analytical data from reorganization energies. IPs are brought down by both alkyl and aryl groups. However, EAs are raised only by aryl units. The results indicate that aryl groups are more helpful in forming excitions for FDDTTP molecules. Consequently, FDDTTP with aryl groups are more efficient acceptor segments for designing donor–acceptor copolymers than those with alkyl groups.

Keywords Intramolecular charge transfer · Photophysical properties · Substituent effect · Theoretical investigation

Electronic supplementary material The online version of this article (doi:10.1007/s00894-012-1438-8) contains supplementary material, which is available to authorized users.

Y. Wang · Q. Peng (✉) · Z. Li · P. He · B. Li
School of Chemical Engineering and Food Science,
Xiangfan University,
Xiangfan 441053, People's Republic of China
e-mail: qiangpengjohnny@yahoo.com

Q. Peng
College of Chemistry, Sichuan University,
Chengdu 610064, People's Republic of China

Introduction

Donor–acceptor (D–A) conjugated copolymers have attracted considerable academic and technological research attention in the past two decades, especially for applications in organic light emitting devices, photovoltaic cells and organic field-effect transistors [1–12]. Among D–A alternating copolymers, the electron-donating moieties of fluorine [13], thiophene [14–16], cyclopentadithiophene [17], dithieno[3,2-b:2′,3′-D]-pyrrole [18] and indolo[3,2-b]carbazole [19] have been investigated widely as donor segments in polymer backbones. These copolymers have attracted particular interest because of the formed intramolecular charge transfer (ICT) [20–23] interaction between the electron donor and acceptor units that can facilitate manipulation of their electronic structures (HOMO/LUMO levels), electronic and optoelectronic properties. To explore and design D–A alternating copolymers with improved performance, it is important to perform the theoretical calculations on their geometries and electronic structures in the ground and excited states. The important parameters including ionization potentials (IPs), electron affinities (EAs), electron-extraction potentials (EEP), hole-extraction potentials (HEP), and reorganization energies (λ), are needed to evaluate the photophysical, carrier injection and transport properties. On the other hand, reorganization energies are also necessary to investigate charge transfer properties.

Recently, thieno[3,4-b]pyrazine (TP) has been found to be a good acceptor unit for the design and preparation of efficient photovoltaic low band gap copolymers [24, 25]. The results of experimental analysis have shown that different substituent groups (methyl and phenyl) in the 2,3-position of TP moiety lead to different effects on the properties of the copolymer [24]. A variety of UV–vis absorptions and fluorescences are achieved by changing different substituent

groups on the TP unit. It is well known that the properties of copolymers correlate with their corresponding monomers. A comprehensive theoretical understanding of the electronic and photophysical properties of D–A monomers will be helpful to further predict the energy levels, optical and other properties of their copolymers with the same repeat segments [26, 27].

In this work, the influences produced by the substituent groups were investigated systematically with the monomer of 9,9′-diethylhexylfluorene-alt-5,7-dithien-2-yl-thieno[3,4-b] pyrazine (FDDTTP). The theoretical models of FDDTTP-H, FDDTTP-Me, FDDTTP-Bu, FDDTTP-Ph, FDDTTP-Bph, and their structures, are shown in Fig. 1. The density functional theory (DFT) method was employed here for calculation of ground-state electronic structures, and time-dependent DFT (TD-DFT) was used to study optical properties. In addition, the energies of HOMO and LUMO levels, the variation in band gaps, charge transfer, absorption wavelengths and emission wavelengths of FDDTTP-R (here, R groups are shortened form of hydrogen atom, methyl, n-butyl, phenyl, and biphenyl unit, respectively) were calculated in this work, and we made a point of exploring the effects of the substituent side groups on the electronic and photophysical properties of the model compounds.

Computational details

The ground geometries and electronic structures of the model compounds were optimized in the gas phase by the hybrid DFT method at the B3LYP level of theory (Becke's three parameter functional and the Lee-Yang-Parr functional) with 6-31G(d) basis set [28–30]. Ground geometries were also optimized in the gas phase by CAM-B3LYP with 6-31G(d). Geometry optimizations of the first lowest singlet states were performed using a TD-B3LYP [31–33]/6-311++G(d,p) approach. The integral equation formalism of the polarizable continuum model (PCM) was employed [34, 35]. Vibrational frequencies were calculated at the same theoretical level to confirm that all optimized ground configurations had no imaginary frequencies and were minima on potential energy surfaces. The relative zero point energies of the ground geometries are listed in Table S1. Properties, including HOMO/LUMO energies, IPs/EAs, HEP, EEP, λ and band gaps, were derived from single point energy calculations performed at B3LYP/6-31G(d) level and compared with experimental results when available [24]. Based on the optimized structures, atomic charges were computed using natural population analysis. On the basis of ground-state and the first singlet excited-state optimizations, the TD-DFT approach was applied to investigate the excited-state electronic properties. All calculations on the monomers in this work were performed with the Gaussian 09 program [36].

Results and discussion

Geometric parameters and properties

The main optimized geometry parameters including dihedral angle (φ), bridge bond length (L_B) and carbon–carbon bond length of donors of FDDTTP-H, FDDTTP-Me, FDDTTP-Bu, FDDTTP-Ph, FDDTTP-Bph by B3LYP/6-31G(d) are shown in Fig. S1. In Fig. S1, we compare excited structures (S_1) with ground structures (S_0). The optimized geometry parameters for the five model compounds by CAM-B3LYP/6-31G(d) and B3LYP/6-31G(d) are listed in Table S2. Comparison between the optimized geometries of the five model compounds obtrained using the two methods reveals quite similar features. As shown in Fig. S1, the dihedral angle (φ) (labeled in Fig. 1) is the deviation from coplanarity between thiophene and TP. Here, L_B (labeled in Fig. 1) refers to the

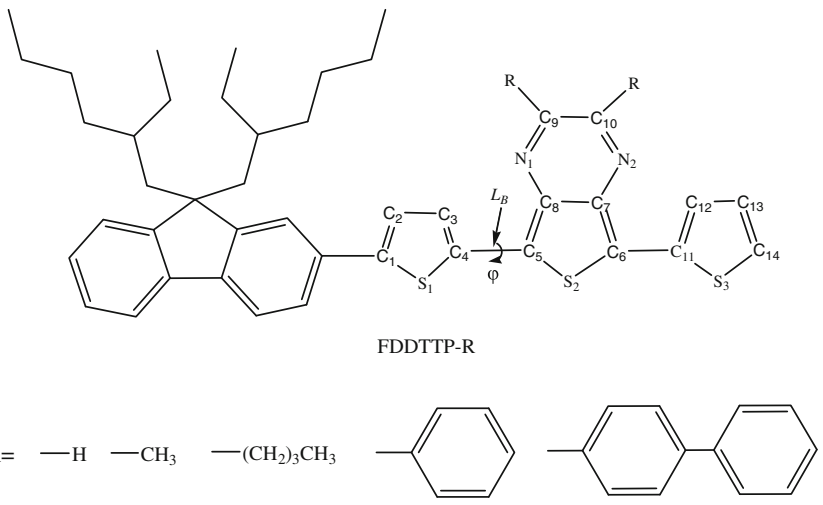

Fig. 1 Structures of 9,9′-diethylhexylfluorene-alt-5,7-dithien-2-yl-thieno[3,4-b] pyrazine (FDDTTP) derivatives FDDTTP-H, FDDTTP-Me, FDDTTP-Bu, FDDTTP-Ph, FDDTTP-Bph

bond length between thiophene and the TP unit in the center of the molecule.

In none of the model compounds is the whole molecule planar. With increasing lengths of alkyl and aryl side chains, the dihedral angles become smaller. Due to both the electron-withdrawing inductive effects of alkyl groups and the obvious electron-withdrawing conjugated effects of aryl groups, the conjugated effects of D–A fragments in FDDTTP-R are undermined in the ground state. The L_B of the five molecules is 1.435 or 1.434 Å. This indicates that the lengths of alkyl and aryl groups have little effect on L_B of FDDTTP-H, FDDTTP-Me, FDDTTP-Bu, FDDTTP-Ph and FDDTTP-Bph.

As shown in Fig. S1, the optimized geometry structures results show that all the D–A fragments in the FDDTTP-H, FDDTTP-Me, FDDTTP-Bu, FDDTTP-Ph and FDDTTP-Bph exhibit closed planar structures because the dihedral angles are nearly 180°. We can predict differences in the bond lengths between the S_0 and S_1 from molecular orbitals (MO) nodal patterns (see section on Frontier molecular orbitals). Bond lengths with bonding character in HOMO but antibonding character in LUMO lengthen upon excitation. On the contrary, the bond lengths will be shortened. The bridge bonds rotate to some extent when excited from the ground state to the excited state. In all five molecules studied, the excited structures have a strong coplanar tendency.

The bond lengths of C_9–C_{10} in FDDTTP-Me, FDDTTP-Bu, FDDTTP-Ph and FDDTTP-Bph are longer than that in FDDTTP-H, which indicates that the substituent side groups have a marked influence on bond length in the model compounds. Both the electron-withdrawing inductive effects of the alkyl groups and the electron-withdrawing conjugated effect of aryl groups can weaken the conjugation of the D–A fragments in FDDTTP molecules. The reason can be attributed to the longer length of bond C_9–C_{10} in FDDTTP with longer length of alkyl and aryl in the ground and excited states, and the steric effects of the longer C_9–C_{10} bond length.

Frontier molecular orbitals

The HOMOs, LUMOs, and energy gaps are related to optical and electronic properties. The largest oscillator strength always leads to the strongest electron transition, which corresponds exclusively to promotion of an electron from HOMO to LUMO (see section on Absorption and emission spectra in solution). The contours of the frontier orbitals (HOMO and LUMO) of all molecules by B3LYP/6-31G(d) were plotted in Fig. 2. The energies of the frontier molecular orbitals, HOMO−LUMO gaps (ΔE) and the lowest excitation energies (E_g) by CAM-B3LYP/6-31G(d) and B3LYP/6-31G(d) are listed in Fig. 3 and Table S3, respectively. From the results summarized in Table S3 and Fig. 3, it appears clear that B3LYP/6-31G(d) leads to more accurate frontier orbitals and transition energies than those obtained using CAM-B3LYP/6-31G(d). In order to observe the variation in HOMOs, LUMOs and energy gaps vividly, the density of state (DOS) of each model compound is shown in Fig. S2.

Figure 2 shows that all frontier orcbitals in the molecules spread over the π-conjugated backbone, and that there is a small contribution from the 9,9′-diethylhexylfluorene (F) part. There is anti-bonding between the bridge atoms of the inter-ring, and there is bonding between the bridge carbon atoms and its conjoint atoms of the intra-ring in the HOMO. However, there is bonding in the bridge single bond of the inter-ring, and antibonding between the bridge atom and its neighbor of the intra-ring in the LUMO.

The distribution of frontier orbital energy levels calculated (from HOMO-5 to LUMO+5) for all the model compounds is displayed in Fig. 3. As can be seen, the calculated HOMO/LUMO energies of FDDTTP-Me and FDDTTP-Ph are in agreement with reported values [24]. Figure S2 shows the ΔE of the five monomers in vacuum. As shown in Figs. 3 and S2, The $\Delta E/E_g$ of FDDTTP-Me and FDDTTP-Ph are 2.29 eV/2.02 eV and 2.16 eV/1.86 eV, cf. the experimental data of $\Delta E/E_g$ of 1.81 eV/1.61 eV and 1.74 eV/1.55 eV. The experimental values [24] of the $\Delta E/E_g$ and the HOMO/LUMO energies of FDDTTP-Me and FDDTTP-Ph exhibit some deviation from the calculated data. The reason is that polarization effects and intermolecular packing forces have been neglected in the calculation treatments. Obviously, the ΔE and E_g of the FDDTTP with the aryl substituent groups are smaller than those of FDDTTP-H. On the contrary, the ΔE and E_g of the FDDTTP with the alkyl group are greater than FDDTTP-H. The results indicate that the ΔE can be brought down by the intense π-conjugated interaction, which is in accordance with the measured shifted absorption spectra with the substituent groups [24]. It is also can be seen from Figs. 3 and S2 that the negative energies of HOMO and LUMO become smaller when introducing the substituent aryl or alkyl group.

Ionization potential, electron affinity and reorganization energy

The adequate and balanced transports of both injected electrons and holes are important in optimizing the device performances of donor-acceptor conjugated copolymers for light-emitting diodes. The ionization potential (IP) and electron affinity (EA) are well-defined properties that can be calculated to estimate the energy barriers for judging the level of ease or difficulty for carrier injection. The IP and EA can be either for vertical excitations (v, at the geometry of the neutral molecule) or

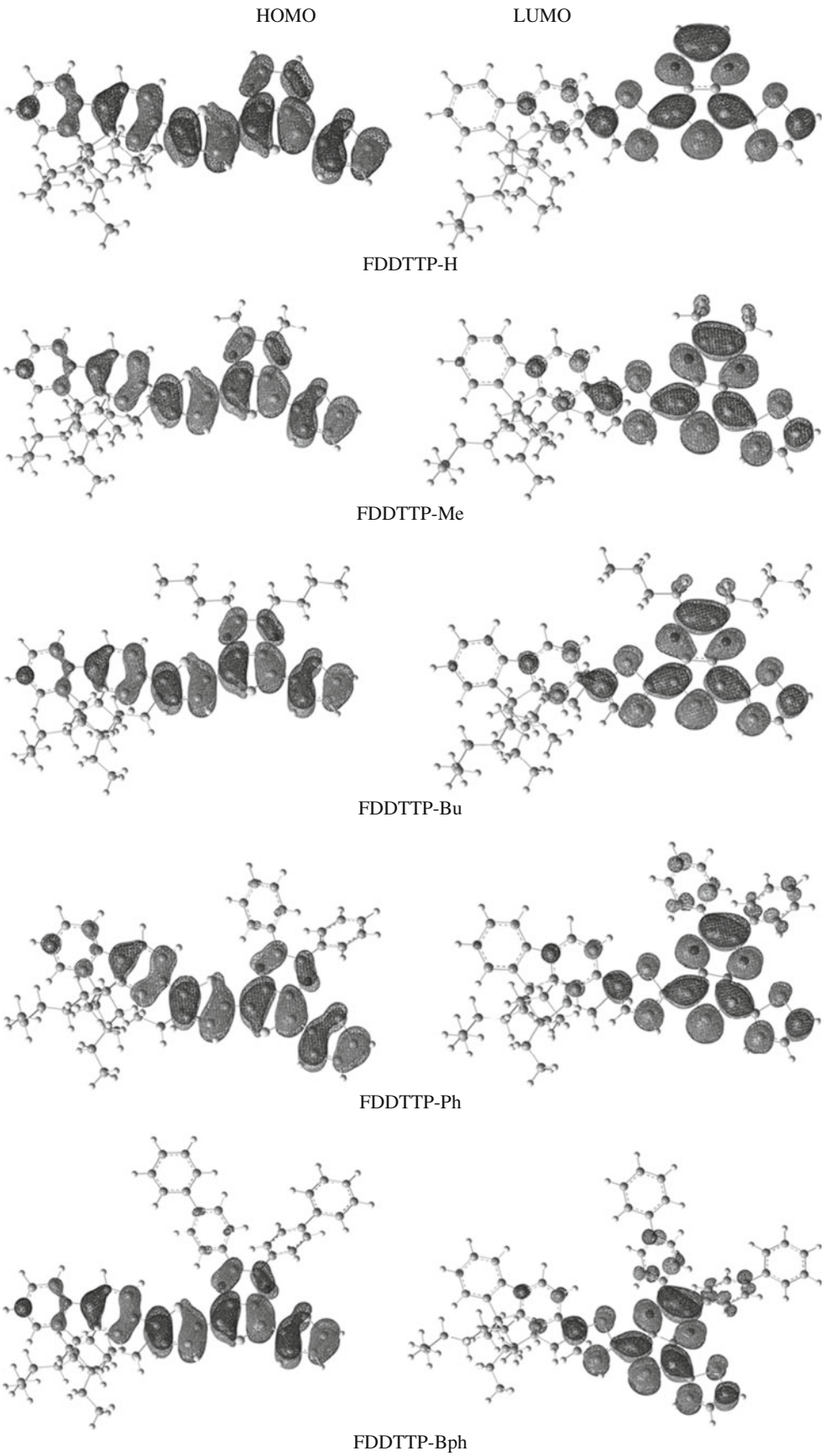

Fig. 2 Contour plots of HOMO and LUMO orbitals of FDDTTP, FDDTTP-Me, FDDTTP-Bu, FDDTTP-ph, FDDTTP-Bph at the B3LYP/6-31G(d) level

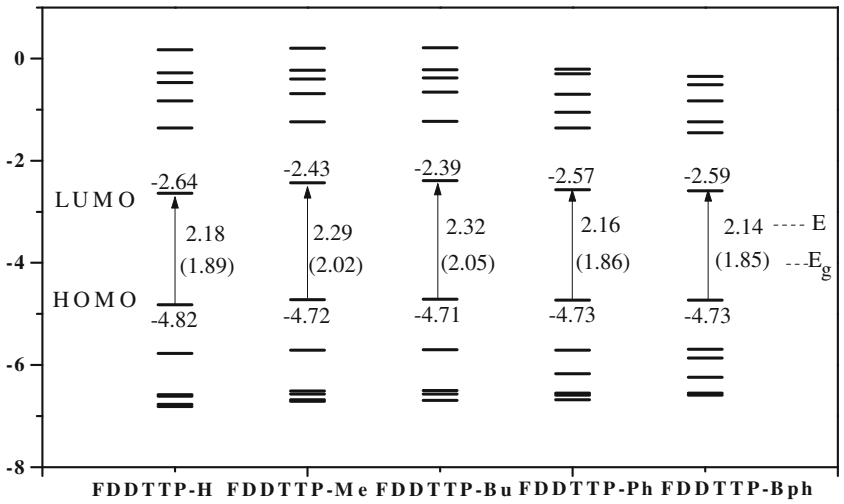

Fig. 3 Diagrams of energy levels of some frontier molecular orbitals, ΔE by DFT and E_g by TD-DFT for all monomers (ΔE and E_g are given in eV)

adiabatic excitations (*a*, optimized structure for both the neutral and charged molecule). In addition, HEP is the energy difference from E (neutral molecule) to E^+ (cationic), with using E^+ geometric structure in calculation, and EEP is the energy difference from E to E^- (anionic), with using E^- geometric structure in calculation. The calculated IPs(v, a), EAs(v, a), HEP, EEP and $\lambda_{hole/electron}$ are listed in Table 1.

As shown in Table 1, the adiabatic and vertical energies of FDDTTP-H required to extract an electron from the neutral molecule are 5.66 and 5.81 eV, while the $EA_{(a/v)}$ energies needed to create a hole are nearly 1.41 and 1.26 eV. The IP(v/a) energies of FDDTTP-Me, FDDTTP-Bu, FDDTTP-Ph, FDDTTP-Bph reduce as the length off alkyl and aryl substituent groups grows. The *EA*(v/a) energies of 1.42/1.54 eV and 1.26/1.40 eV for FDDTTP-Me and FDDTTP-Bu reduce with the growing lengths of alkyl groups, while the *EA*(v/a) energies of 1.49/1.62 eV and 1.58/1.69 eV for FDDTTP-Ph and FDDTTP-Bph increase with the length of aryl groups. The above results indicate that it is easy to form excitions with the aryl substituent group on the acceptor moiety, and FDDTTP-Bph is more favorable for hole-creating and electron-accepting than the other molecules.

The charge mobility in organic molecular materials is usually described with Marcus electron transfer theory [37]. The charge (hole or electron) transfer rate K can be expressed by the following formula [38, 39]:

$$K_{hole/electron} = \frac{4\pi^2}{h}\Delta H_{ab}{}^2 \frac{1}{\sqrt{4\pi\lambda_{hole/electron}T}} \exp\left(\frac{\lambda_{hole/electron}}{4K_bT}\right) = A\exp\left(-\frac{\lambda_{hole/electron}}{4K_bT}\right) \quad (1)$$

Here, ΔH_{ab} is the electronic coupling matrix element between the donor and acceptor molecules, $\lambda_{hole/electron}$ is the reorganization energy for hole/electron transport, h is Planck's constant, and k is Boltzman's constant. In particular, the ΔH_{ab} and k terms play an important role in determining $K_{hole/electron}$. However, it is most likely that ΔH_{ab} would vary over a limited range for analogous molecules [40–42].

The mobility of charges has been demonstrated to be related dominantly to the internal reorganization energy $\lambda_{hole/electron}$ for organic light-emitting diodes. The $\lambda_{electron}$ is electron reorganization energy, which can be expressed as follows:

$$\lambda_{electron} = \lambda_0 + \lambda_- = \left(E_0^* - E_0\right) + \left(E_-^* - E_-\right) = EEP - EA_{(v)} \quad (2)$$

where E_0 and E_- are the energies of the neutral and anion species in their lowest energy geometries, while E_0^* and E_-^*

Table 1 Ionization potential (IP), electron affinity (EA), hole-extraction potentials (HEP), electron-extraction potentials (EEP), and reorganization energies (λ) λ_{hole} and $\lambda_{electron}$ for series molecules

Energy (eV)	IP(a)[b]	IP(v)	HEP	EA(v)	EA(a)	EEP	λ_{hole}	$\lambda_{electron}$
FDDTTP-H	5.66	5.81	5.53	1.26	1.41	1.53	0.28	0.13
FDDTTP-Me	5.78	5.92	5.63	1.42	1.54	1.68	0.29	0.14
FDDTTP-Bu	5.63	5.77	5.47	1.26	1.40	1.55	0.30	0.15
FDDTTP-Ph	5.61	5.75	5.48	1.49	1.62	1.74	0.27	0.12
FDDTTP-Bph	5.58	5.71	5.45	1.58	1.69	1.80	0.26	0.11

[b] (*v*) vertical excitations, (*a*) adiabatic excitations

Table 2 Electronic transition data obtained by time-dependent density functional theory (TD-DFT) in $CHCl_3$

Molecule	Electronic transitions	λ(nm)	$\lambda^{a}{}_{exp}$(nm)	*f*	Main configurations
FDDTTP-H	$S_0 \rightarrow S_1$	675		0.590	H→L (79 %)
	$S_0 \rightarrow S_3$	418		0.899	H→L+1 (89 %)
FDDTTP-Me	$S_0 \rightarrow S_1$	637	412/588	0.765	H→L (81 %)
	$S_0 \rightarrow S_3$	410		0.790	H→L+1 (85 %)
FDDTTP-Bu	$S_0 \rightarrow S_1$	621		0.798	H→L (79 %)
	$S_0 \rightarrow S_3$	411		0.700	H→L+1 (80 %)
FDDTTP-Ph	$S_0 \rightarrow S_1$	689	425/639	0.560	H→L (80 %)
	$S_0 \rightarrow S_3$	427		0.799	H→L+1 (89 %)
FDDTTP-Bph	$S_0 \rightarrow S_1$	695		0.499	H→L (78 %)
	$S_0 \rightarrow S_4$	441		0.500	H→L+1 (76 %)

represent the energies of the neutral and anion molecules with the geometries of the anion and neutral molecules, which is equal to the difference between vertical $EA_{(v)}$ and EEP.

Likewise, λ_{hole} for hole transfer can be expressed as follows:

$$\lambda_{hole} = \lambda_0 + \lambda_+ = \left(E_0^* - E_0\right) + \left(E_+^* - E_+\right) = IP_{(v)} - HEP \quad (3)$$

The data in Table 1 show that the λ_{hole} values for FDDTTP-H, FDDTTP-Me, FDDTTP-Bu, FDDTTP-Ph and FDDTTP-Bph are all bigger than their corresponding $\lambda_{electron}$ values, which indicates that the electron transfer rate is higher than the hole transfer rate. According to the values listed in Table 1, these molecules can be used as hole/electron transporters. It also shows that various substituent groups produce a tremendous influence on the reorganization energy of FDDTTP. The reorganization energy is increased by alkyl groups, and is reduced gradually by aryl groups. Hence, aryl groups are more beneficial to the formation of intramolecular charge transfer than alkyl groups.

Absorption and emission spectra in solution

We used continuous medium theory to perform calculations for solvent effects in our work. Transition energies of the excited states of FDDTTP-H, FDDTTP-Me, FDDTTP-Bu, FDDTTP-Ph, FDDTTP-Bph in $CHCl_3$ were computed using the PCM model linked to TD-DFT (B3LYP) with the 6-311+G(d,p) basis sets. The overall solution effects on geometry are negligible. The singlet excited states of the five molecules were calculated at the optimized structure of the ground state in solution for each species. The absorption and emission wavelengths (λ) in the S_1, the oscillator strength (*f*) and the

Table 3 Emission spectra obtained by TDDFT in $CHCl_3$

Molecule	Electronic transitions	λ(nm/eV)	*f*	Main configurations
FDDTTP-H	$S_1 \rightarrow S_0$	915(1.37)	0.639	H←L (98 %)
FDDTTP-Me	$S_1 \rightarrow S_0$	849(1.47)	0.769	H←L (96 %)
FDDTTP-Bu	$S_1 \rightarrow S_0$	799(1.54)	0.702	H←L (97 %)
FDDTTP-Ph	$S_1 \rightarrow S_0$	921(1.36)	0.580	H←L (96 %)
FDDTTP-Bph	$S_1 \rightarrow S_0$	929(1.35)	0.545	H←L (98 %)

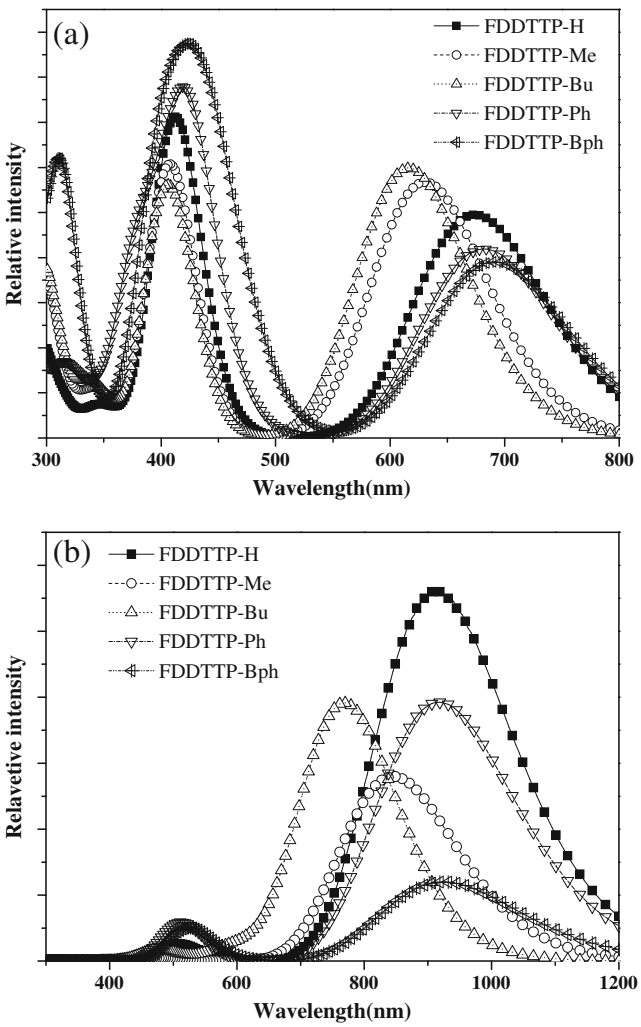

Fig. 4 Gaussian-type absorption (**a**) and emission (**b**) spectra in $CHCl_3$ solvent

main configurations of corresponding excited states are listed in Tables S4 and S5. The calculated absorption and emission spectra of FDDTTP-H, FDDTTP-Me, FDDTTP-Bu, FDDTTP-Ph and FDDTTP-Bph by TDDFT are simulated in Fig. S3. The transition energies, *f* and main configurations for most relevant singlet excited states in solution are listed in Tables 2 and 3. The corresponding absorption and emission spectra are described in Fig. 4.

The calculated maximum absorption peaks in $CHCl_3$ solution exhibit some red shifts compared to the results in gas phase for FDDTTP-H, FDDTTP-Me, FDDTTP-Bu, FDDTTP-Ph, FDDTTP-Bph (described in Table 2, Figs. S3a and Fig. 4a). The maximum absorption wavelengths in $CHCl_3$ solution are larger than those in gas phase, which indicates that the solvent effects stabilize the excited state, inducing the red shift of the absorption spectra. The absorption wavelength is progressively blue-shifted gradually with the increase in alkyl length, but red-shifted with the increase in aryl group length. The influence of $CHCl_3$ on the emission spectra of FDDTTP-H, FDDTTP-Me, FDDTTP-Bu, FDDTTP-Ph, FDDTTP-Bph (described in Table 3, Figs. S3b and Fig. 4b) was also calculated using the PCM model. The results indicate that the solvent can stabilize the excited states for FDDTTP-H, FDDTTP-Me, FDDTTP-Bu, FDDTTP-Ph, FDDTTP-Bph. The maximum emission wavelengths in $CHCl_3$ are larger than those in the gas phase, giving rise to the red shift, which is coincident with that observed in absorption spectra. The aryl and alkyl groups afford the same influence in gas and solution in this work. The data listed in Table 2 show that the TD-DFT results deviate from the observed experimental absorption spectra. The reason can be attributed to the different media, the drawbacks of TD-DFT itself, and so on.

Conclusions

A comprehensive investigation was performed to explore the effects of the different substituent groups on FDDTTP. The calculated results show that optical and electronic properties, including HOMOs, LUMOs, ΔE, IPs, EAs, $\lambda_{hole/electron}$, absorption and emission spectra, are affected by different substituent groups. Variations in φ were also calculated, which illustrate that the electronic effects of the substituent groups clearly influence the molecular structures in both the ground and excited states. Because of the electron-donating effects of the phenyl and biphenyl groups, all the model compounds show better electron transport properties than the hole transport property, especially for the FDDTTP-Bph with minimum λ_{hole} and $\lambda_{electron}$ of 0.26 and 0.11 eV, respectively. The investigation of IP and EA shows that the studied molecules with the aryl substituent are helpful to form excitions including electron and hole. The lowest-lying absorptions of FDDTTP-Ph and FDDTTP-Bph based on the optimized geometry structures in the ground states have bathochromic shifts compare to FDDTTP-H. However, the lowest-lying absorptions of FDDTTP-Me and FDDTTP-Bu have hypsochromic shifts compare to FDDTTP-H. The spectrum properties of the donor–acceptor molecules can be modified by just fine-tuning the substituent side groups on the acceptor, which provides a theoretical support for the design of donor-acceptor copolymers for light-emitting materials. In brief, calculations predict that the favorable character of the monomers and their corresponding copolymers with aryl-substituent groups can be used as light-emitting materials.

Acknowledgments The work was supported financially by the Natural Science Foundation of China (No: 20802033), Program for New Century Excellent Talents in University (No: NCET-10-0170), Yong Scientist of Jing Gang Zhi Xing Project of Jiangxi Province (No: 2008DQ00700), Natural Science Foundation of Jiangxi Province (No: 2010GZH0110) and Scientific Research Foundation of Hubei Provincial Education Department (No: D20112603, Q20112607) and Xiangfan University (No: 2010YA010).

References

1. Segalman RA, McCulloch B, Kirmayer S, Urban JJ (2009) Macromolecules 42:9205–9216
2. Grimsdale AC, Chan KL, Martin RE, Jokisz PG, Holmes AB (2009) Chem Rev 109:897–1091
3. Inganäs O, Zhang F, Andersson MR (2009) Acc Chem Res 42:1731–1739
4. Sonar P, Singh SP, Leclere P, Surin M, Lazzaroni R, Lin TT, Dodabalapur A, Sellinger A (2009) J Mater Chem 19:3228–3237
5. Guenes S, Neugebauer H, Sariciftci NS (2007) Chem Rev 107:1324–1338
6. Cheng YJ, Yang SH, Hsu CS (2009) Chem Rev 109:5868–5923
7. Kulkarni AP, Zhu Y, Jenekhe SA (2005) Macromolecules 38:1553–1563
8. Li C, Liu MY, Pschirer NG, Baumgarten M, Müllen K (2010) Chem Rev 110:6817–6855
9. Beaujuge PM, Reynolds JR (2010) Chem Rev 110:268–320
10. Xin H, Kim FS, Jenekhe SA (2008) J Am Chem Soc 130:5424–5425
11. Blouin N, Michaud A, Gendron D, Wakim S, Blair E, Neagu-Plesu R, Belletete M, Durocher G, Tao Y, Leclerc M (2008) J Am Chem Soc 130:732–742
12. Pang H, Skabara P, Crouch DJ, Duffy W, Heeney M, McCulloch I, Coles SJ, Horton PN, Hursthouse MB (2007) Macromolecules 40:6585–6593
13. Peng Q, Xu J, Li MJ, Zheng WX (2009) Macromolecules 42:5478–5485
14. Baek NS, Hau SK, Yip HL, Acton O, Chen KS, Jen AKY (2008) Chem Mater 20:5734–5736
15. Liu CL, Tsai JH, Lee WY, Chen WC, Jenekhe SA (2008) Macromolecules 41:6952–6959
16. Peng Q, Park K, Lin T, Durstock M, Dai LM (2008) J Phys Chem B 112:2801–2808
17. Moulè AJ, Tsami A, Bünnagel TW, Forster M, Kronenberg NM, Scharber M, Koppe M, Morana M, Brabec CJ, Meerholz K, Scherf U (2008) Chem Mater 20:4045–4050
18. Zhou EJ, Nakamura M, Nishizawa T, Zhang Y, Wei QS, Tajima K, Yang CH, Hashimoto K (2008) Macromolecules 41:8302–8305

19. Peng Q, Liu XJ, Qin YC, Li MJ, Xu J, Fu GW, Dai LM (2011) J Mater Chem 21:7714–7722
20. Coropceanu V, Cornil J, Da Silva DA, Olivier Y, Silbey R, Bredas JL (2007) Chem Rev 107:926–952
21. Tsai FC, Chang CC, Liu CL, Chen WC, Jenekhe SA (2005) Macromolecules 38:1958–1966
22. Peng Q, Lu ZY, Huang Y, Xie MG, Xiao D, Han SH, Peng JB, Cao Y (2004) J Mater Chem 14:396–401
23. Liu CC, Tsai FC, Chang CC, Hsieh KH, Lin JJ, Chen WC (2005) Polymer 46:4950–4957
24. Zhou EJ, Cong J, Yamakawa S, Wei Q, Nakamura M, Tajima K, Yang C, Hashimoto K (2010) Macromolecules 43:2873–2879
25. Peng Q, Liu XJ, Qin YC, Zhou D, Xu J (2011) J Polym Sci A Polym Chem 49:4458–4467
26. Wang YL, Peng Q, Hou QF, Zhao K, Liang Y, Li BL (2011) Theor Chem Acc 129:257–270
27. Riobe F, Grosshans P, Sidorenkova H, Geoffroy M, Avarvari N (2009) Chem A Eur J 15:380–395
28. Becke AD (1988) Phys Rev A 38:3098–3100
29. Becke AD (1993) J Chem Phys 98:5648–5652
30. Lee C, Yang W, Parr RG (1988) Phys Rev B 37:785–789
31. Dreuw A, Head-Gordon M (2005) Chem Rev 105:4009–4037
32. Barone V, Polimeno A (2007) Chem Soc Rev 36:1724–1731
33. Jacquemin D, Mennucci B, Adamo C (2011) Phys Chem Chem Phys 13:16987–16998
34. Tomasi J, Cammi R, Mennucci B, Cappelli C, Corni S (2002) Phys Chem Chem Phys 24:5697–5703
35. Cossi M, Barone V (2001) J Chem Phys 115:4708–4717
36. Frisch MJ, Trucks GW, Schlegel HB, Scuseria GE, Robb MA, Cheeseman JR, Scalmani G, Barone V, Mennucci B, Petersson GA, Nakatsuji H, Caricato M, Li X, Hratchian HP, Izmaylov AF, Bloino J, Zheng G, Sonnenberg JL, Hada M, Ehara M, Toyota K, Fukuda R, Hasegawa J, Ishida M, Nakajima T, Honda Y, Kitao O, Nakai H, Vreven T, Montgomery JJA, Peralta JE, Ogliaro F, Bearpark M, Heyd JJ, Brothers E, Kudin KN, Staroverov VN, Kobayashi R, Normand J, Raghavachari K, Rendell A, Burant JC, Iyengar SS, Tomasi J, Cossi M, Rega N, Millam JM, Klene M, Knox JE, Cross JB, Bakken V, Adamo C, Jaramillo J, Gomperts R, Stratmann RE, Yazyev O, Austin AJ, Cammi R, Pomelli C, Ochterski JW, Martin RL, Morokuma K, Zakrzewski VG, Voth GA, Salvador P, Dannenberg JJ, Dapprich S, Daniels AD, Farkas O, Foresman JB, Ortiz JV, Cioslowski J, Fox DJ (2009) Gaussian 09, Revision A.02. Gaussian, Inc, Wallingford
37. Hutchison GR, Ratner MA, Marks TJ (2005) J Am Chem Soc 127:2339–2350
38. Marcus RA, Sutin N (1985) Biochim Biophys Acta 811:265–322
39. Marcus RA (2000) J Electroanal Chem 483:2–6
40. Coropceanu V, Gruhn NE, Barlow S, Lambert C, Durivage JC, Bill TG, Nöll G, Marder SR, Brédas JL (2004) J Am Chem Soc 126:2727–2731
41. Nelsen SF, Trieber DA II, Ismagilov RF, Teki Y (2001) J Am Chem Soc 123:5684–5694
42. Wang YL, Peng Q, Liang Y, Li BL, Zhu WG (2011) Aust J Chem 64:1475–1484